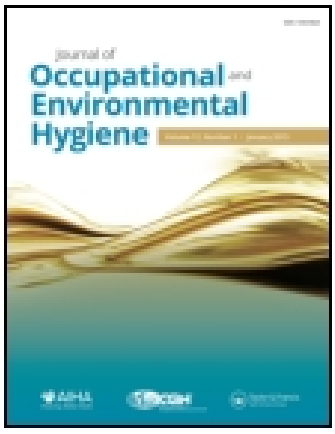

Journal of Occupational and Environmental Hygiene
Publication details, including instructions for authors and subscription information:
http://www.tandfonline.com/loi/uoeh20

Effects of Data Sparsity and Spatiotemporal Variability on Hazard Maps of Workplace Noise

Kirk Lake[a], Jun Zhu[b], Haonan Wang[c], John Volckens[a] & Kirsten A. Koehler[d]

[a] Department of Environmental and Radiological Health Sciences, Colorado State University, Fort Collins, Colorado

[b] Department of Statistics and Department of Entomology, University of Wisconsin, Madison, Wisconsin

[c] Department of Statistics, Colorado State University, Fort Collins, Colorado

[d] Department of Environmental Health Sciences, Johns Hopkins Bloomberg School of Public Health, Baltimore, Maryland

Accepted author version posted online: 01 Dec 2014.Published online: 04 Mar 2015.

To cite this article: Kirk Lake, Jun Zhu, Haonan Wang, John Volckens & Kirsten A. Koehler (2015) Effects of Data Sparsity and Spatiotemporal Variability on Hazard Maps of Workplace Noise, Journal of Occupational and Environmental Hygiene, 12:4, 256-265, DOI: 10.1080/15459624.2014.963589

To link to this article: http://dx.doi.org/10.1080/15459624.2014.963589

Journal of Occupational and Environmental Hygiene, 12: 256–265
ISSN: 1545-9624 print / 1545-9632 online

DOI: 10.1080/15459624.2014.963589

Effects of Data Sparsity and Spatiotemporal Variability on Hazard Maps of Workplace Noise

Kirk Lake,[1] Jun Zhu,[2] Haonan Wang,[3] John Volckens,[1] and Kirsten A. Koehler[4]

[1]Department of Environmental and Radiological Health Sciences, Colorado State University, Fort Collins, Colorado
[2]Department of Statistics and Department of Entomology, University of Wisconsin, Madison, Wisconsin
[3]Department of Statistics, Colorado State University, Fort Collins, Colorado
[4]Department of Environmental Health Sciences, Johns Hopkins Bloomberg School of Public Health, Baltimore, Maryland

Personal sampling, considered a state-of-the-art technique to assess worker exposures to occupational hazards, is often conducted for the duration of a work shift so that time-weighted average (TWA) exposures may be evaluated relative to published occupational exposure limits (OELs). Such cross-shift measurements, however, provide little information on the spatial variability of exposures, except after a very large number of samples. Hazard maps, contour plots (or similar depiction) of hazard intensity throughout the workplace, have gained popularity as a way to locate sources and to visualize spatial variability of physical and chemical hazards within a facility. However, these maps are often generated from short duration measures and have little ability to assess temporal variability. To assess the potential bias that results from the use of short-duration measurements to represent the TWA in a hazard map, noise intensity measurements were collected at high spatial and temporal resolution in two facilities. Static monitors were distributed throughout the facility and used to capture the temporal variability at these locations. Roving monitors (typical of the hazard mapping process) captured spatial variability over multiple traverses through the facility. The differences in hazards maps generated with different sampling techniques were evaluated. Hazard maps produced from sparse, roving monitor data were in good agreement with the TWA hazard maps at the facility with low temporal variability. Estimated values were within 5 dB of the TWA over approximately 90% of the facility. However, at the facility with higher temporal variability, large differences between hazard maps were observed for different traverses through the facility. On the second day of sampling, estimates were at least 5 dB different than the TWA for more than half of the locations within the facility. The temporal variability of noise was found to have a greater influence on map accuracy than the spatial sampling resolution.

Keywords hazard mapping, noise exposure, spatiotemporal variability

Address correspondence to: Kirsten A. Koehler, 615 N Wolfe St, Baltimore, MD 21205; e-mail: kirsten.koehler@jhu.edu

Color versions of one or more of the figures in the article can be found online at www.tandfonline.com/uoeh.

INTRODUCTION

Workers are exposed to a variety of physical, chemical, and biological hazards. Noise- induced hearing loss (NIHL) is one of the most common forms of occupational disease despite the Occupational Safety and Health Administration's (OSHA) requirements on the use of Hearing Conservation Programs (HCP) to protect workers in industries with hazardous noise levels. Since an estimated 30 million workers are exposed to hazardous noise levels, the National Institute for Occupational Safety and Health (NIOSH) lists hearing loss as one of its 21 priority research areas for the 21st century. [(1)]. Although NIHL is preventable, its effects are permanent; this form of hearing loss cannot be treated with surgery or hearing aids. Short-term exposures to loud noise can lead to cross-shift decrements in hearing and symptoms such as ringing. Repeated or long-term exposures to loud noise can lead to permanent hearing loss making workers especially vulnerable to NIHL. [(2)] Susceptibility to NIHL varies by subject and may worsen with co-exposure to some pharmaceuticals and organic solvents. [(3,4)] A number of non-auditory physiological effects have also been associated with loud noise such as affected blood pressure and blood pressure variation, affected heart rate, reduced rates of breathing, hormonal changes, and brief skeletal-muscle tension. OSHA regulates noise exposure with a permissible exposure limit (PEL) of 90 dBA for a time-weighted average (TWA) over an 8-hr work shift.

Hazard maps, contour plots of hazard concentration over a corresponding two-dimensional floor plan of the workplace,

have gained popularity as a method to visualize the spatial distribution of a hazard intensity throughout a facility. [5–9] With appropriate sampling plans, the sources and extent of hazardous exposures can be determined with a high degree of spatial resolution. Hazard maps provide a great deal of visual information in a format that is easily understood. Well-designed maps serve as powerful tools for communicating risk to colleagues, management, and employees; such maps can inform effective decision-making on exposure control and prevention. [10] Poorly designed hazard maps, on the other hand, are non-representative and may lead to engineering or administrative controls that produce little effect. [11]

Hazard mapping can suffer from three predominant pitfalls: instrument error, data sparsity, and representativeness. [11] Instrument error, which will not be addressed here, results from various issues including the accuracy, precision, and sensitivity of the measurement device. The completeness of a hazard map is directly related to data sparsity; one cannot simultaneously monitor a hazard at all locations and times. In general, maps with higher spatial and temporal sampling resolutions will have more completeness (reduced sparsity). Sparse measurements must be interpolated to produce continuous estimates of hazard intensity through space. Finally, the representativeness of a hazard map is based on the fact that interpolation of spatially and temporally resolved measurements could result in errors of estimation, misrepresenting the actual sample and its variance. Interpolations with better-fitting spatial statistical models generally result in maps with higher representativeness.[5]

The goal of this research is to assess the quality of hazard maps at facilities with different temporal variability under various sampling strategies. Noise intensity data were collected using both static (i.e., monitors that remained stationary and captured a time series of noise intensity) and roving (i.e., monitors that were moved through the facility to capture noise intensity at many locations) noise monitors, and hazard maps were produced with each data type separately. Hazard maps were produced with subsets of the collected data to evaluate the influence of roving sampling spatial resolution. The difference between hazard maps generated from the roving monitor estimates of the TWA noise intensity using short-duration measurements at each facility were compared to the hazard map produced from the TWA measured by the static monitors.

METHODS

Facilities

We measured noise intensity at two facilities with different spatiotemporal variability in noise emissions. The first was a plastics facility located in Colorado. The room where noise intensity was sampled at the plastics facility was rectangular in shape (149 m × 10 m to 14 m) and encompassed an area of about 1950 m^2 (Figure 1). The facility contained a long, rectangular machine, which spanned the length of the room (143 m × 1.5 m). This machine was the only significant source of noise in the room and operated continuously. Noise intensities were measured on three non-consecutive days.

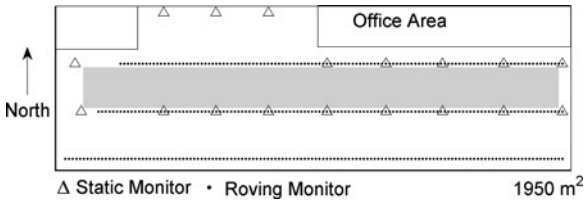

FIGURE 1. Plastics facility floor plan and sampling positions. The machine (noise source) is denoted by the shaded rectangle in the middle of the room. Confined office and other areas are denoted on the north side of the room.

The second facility was an engine testing facility (hereafter "engine facility") also located in Colorado. The area selected for sampling in the engine facility consisted of two rooms, connected lengthwise from north to south by a sliding door. The northern and southern rooms were both rectangular in shape (14.8 m × 6.5 m and 14.8 m x 33.7 m, respectively) and encompassed a combined area of about 595 m^2 (Figure 2). The northern room consisted of an engine test bed on the far west side and a sliding door to the south. Work benches, storage space, and toolboxes filled most of the available wall and floor space; thus, available sampling locations were limited. The southern room contained four large engine test beds and two floor openings leading to the basement below. Major construction activities were occurring directly outside the engine facility during the sampling interval. Noise intensities were monitored on two non-consecutive days at this facility. Engines located in different areas of the facility were tested on each day leading to high temporal and spatial variability.

Noise Monitoring Equipment

Noise intensities were measured at the plastics facility and engine facility facilities with Spark personal dosimeters (Models 706RC and 703, Larson Davis Inc., Provo, UT). All dosimeters were set to log equivalent sound pressure levels (Leq) at 1-sec resolution with the following OSHA required measurement settings: A-weighted, slow response, 5 dB exchange rate. Each dosimeter was calibrated within 24 hr of use with a SparkCal (Model 150, Larson Davis Inc., Provo, UT) at 94 dBA and 114 dBA. Post-calibration revealed no values greater or less than 0.5 dBA from pre-calibration values. The manufacturer specified instrumental accuracy for these instruments was ± 2 dB of the reference value.

Noise Intensity Sampling Strategies

At each facility, a combination of static (i.e., monitors that remained stationary and captured a time series of noise intensity) and roving (i.e., monitors that were moved through the facility to capture noise intensity at many locations) noise monitors were employed to estimate spatial and temporal

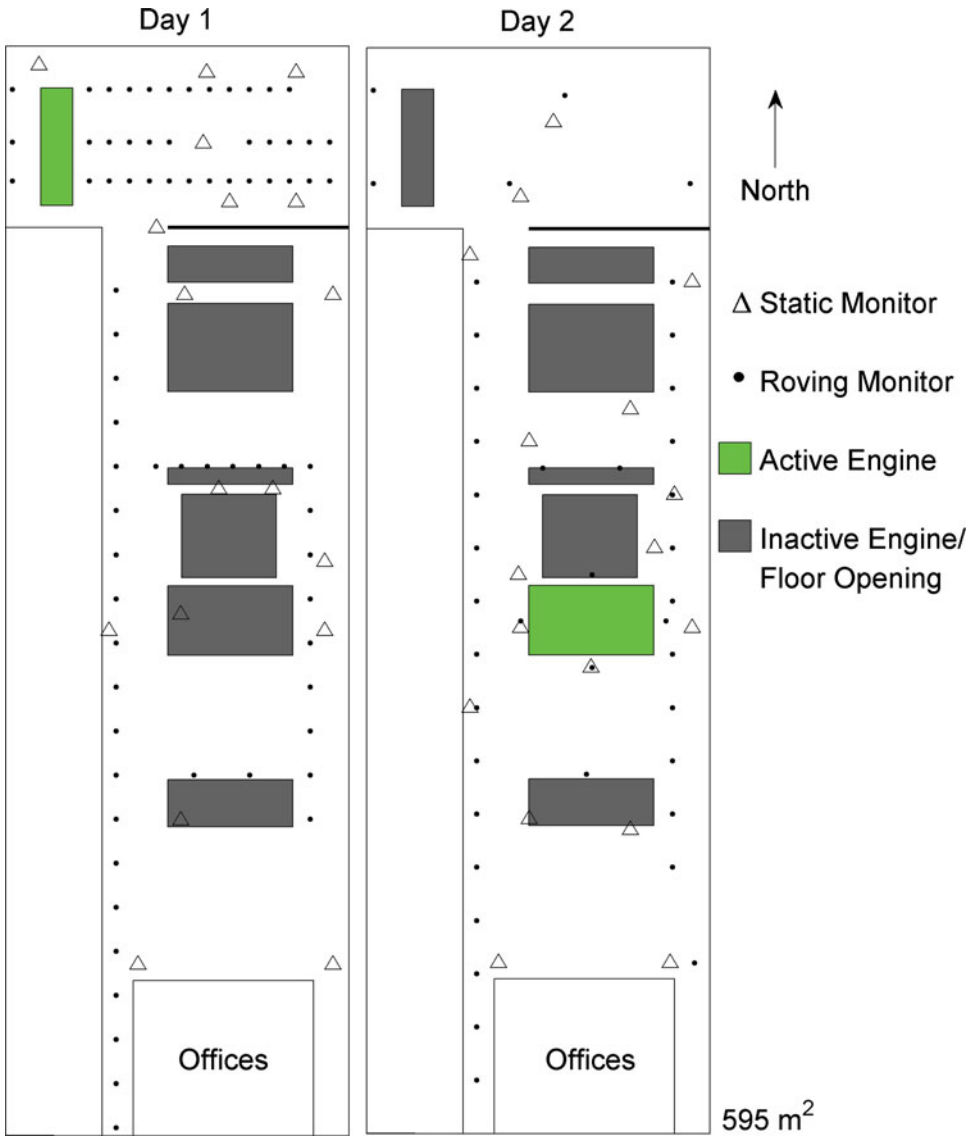

FIGURE 2. The engine facility floor plan with sampling positions for Day 1 and 2. The active engine (noise source) is denoted in green on each day. Inactive engines and open spaces in the floor leading to the basement below are denoted with gray rectangles. Offices flank the west side and south portion of the facility.

variability in noise intensity using the noise dosimeters described above. Up to 20 noise monitors were used each day to produce a comprehensive sample data set; the spatial and temporal coverage of these data sets is considerably higher than what has been typically collected for hazard mapping.

Static Monitoring

Selection of static monitoring positions was based primarily on the number of available monitors and accessibility for monitor placement. Based on the known or predicted locations of noise sources, we attempted to cover the accessible areas of each facility floor plan fairly uniformly, with monitors placed both near and at a distance from known sources. At the plastics facility, personal noise dosimeters were mounted on tripods at hearing zone height (~1.5 m). Eighteen personal noise dosimeters were placed at corresponding positions to the north and south at 1 m distance from the process machine with a 15-m separation distance between meters (Figure 1). Sampling durations exceeded half shifts but did not cover full shifts. At the engine facility, noise dosimeters were mounted at varying (but documented) heights, as dictated by available space. Eighteen noise dosimeters were placed in static positions at the engine facility each day; positions of the static monitors varied by day (Figure 2) because the location of the noise source changed between sampling days. Noise intensities were logged at these positions for 2.5–3 hr per day while engine testing was in progress. Spatial and temporal variability was assessed via empirical cumulative distribution functions of the static monitor data. Data normality was assessed with Shapiro-Wilks tests.

Roving Monitoring

Predetermined, irregular sampling grids were established along accessible areas of each facility. Roving pathways were predetermined according to specified spatial resolution, accessibility, and judgment decisions based on prediction of hazard sources and extent. Personal dosimeter microphones were mounted at shoulder height in the researcher's hearing zones. Two researchers traversed each facility simultaneously. Researcher location was monitored in each facility, relative to a fixed benchmark and with a Lufkin 4 in ABS Plastic and Aluminum Measuring Wheel (Lufkin Industries, Lufkin, TX). Along these predetermined pathways, roving sampling data were collected by a three-step process as follows: first, the researcher stopped at a location, recording the sample start time on the spreadsheet at the corresponding predetermined location entry; second, the researcher waited the allotted sampling duration; and third, the researcher moved to the next location, repeating the steps from the beginning until the sampling was finished.

Roving measurements were collected along three predetermined pathways at the plastics facility (Figure 1). Samples were collected at approximately 1-m resolution for 10-sec per location on each of three sampling days. We estimated that 10 sec was sufficient since noise levels at the plastics facility were at steady-state. [12] The first pathway started in the southeastern corner of the room and followed a western course staying approximately 0.5 m from the southern wall. The second pathway started at the eastern end of the room and followed a western course staying approximately 0.5 m from the southern side of the machine. The third pathway started in the northeastern corner of the room and followed a western course staying approximately 0.5 m from the northern side of the machine. Start times for each 10-sec sampling period were noted on a spreadsheet that was subsequently synchronized to the dosimeter timestamp.

Due to differences in noise source location by day, the roving sampling plan was different for each sampling day at the engine facility (Figure 2). On Day 1 at the engine facility, three separate roving pathways were selected, running from west to east at 1-m resolution in the northern room. In the southern room samples were collected at available areas. Roving measurements were not completed down the southeastern narrow corridor or in the space between the southern-most engine and the office space because this area was being used for storage and not readily accessible, though open to the room. On Day 2 at the engine facility, the only major identifiable source of noise was emitted from an engine in the southern room; roving samples were collected primarily in the southern room with several additional samples collected in the northern room.

Roving measurements were downloaded from the dosimeters and a custom Matlab script (Mathworks, Inc., Natick, MA) was written to extract individual measurements from these files based on recorded start times and known sample durations. Data normality was assessed with Shapiro-Wilks tests.

Hazard Mapping

In the present study ordinary Kriging was utilized to interpolate data for each hazard map at 1 m^2 resolution. Kriging is a geostatistical method for predicting (interpolating) values at unobserved locations and for quantifying the associated uncertainty using prediction standard error, based on a combinations of observed values that are weighted by proximity to the interpolation location (i.e.,, nearby locations are given larger influence in the estimation). [13] In Kriging, a variogram is used to describe spatial dependence as a function of distance between sampling locations. A variogram model is then fit to the observed variogram to calculate appropriate weights for subsequent spatial predictions. We evaluated variogram models and found that a spherical variogram represented the spatial dependence adequately for both the plastics facility and the engine facility. It is common in hazard mapping to predict values for the whole facility beyond the extent of the monitors. [6,8,14] Kriging (compared to simpler interpolation methods) statistically accounts for spatial correlation in the data. Thus, if the correlation holds beyond the extent of the data sites, it is statistically valid to assume that Kriging will provide reasonable estimates, at least for relatively short distances were the spatial correlation is positive. Thus we do not see this as a strong limitation of the method.

All hazard maps and calculations were completed using MATLAB software.

At each facility we calculated the TWA (during active sampling) from the stationary monitors to produce a TWA hazard map for each day. Measurements from roving monitors were used separately to produce multiple hazard maps on each day. Due to the size and spatial density (approximately 385 sampling locations per traverse) of the roving measurement campaign at the plastics facility, each of two researchers generated one or two complete traverses through the facility on each day. As such, a subset of observations was drawn at random from each traverse and used for hazard map generation. Four levels of resolution were considered at the plastics facility (N = 385, 100, 50, or 25; corresponding to 1 sample every 5, 20, 39, or 78 m^2). At the engine facility, a full traverse consisted of 75 sampling locations on Day 1 (noise intensity measured in both rooms) and 30 sampling locations on Day 2 (focusing primarily in the larger, southern room). Given the smaller size of the engine facility, the spatial sampling resolution was also reduced (N = 75 for Day 1 or 30 for Day 2, 15, or 8; corresponding to 1 sample every 8 on Day 1 or 20 on Day 2, 40, or 75 m^2). Under this experimental design, the low-resolution cases at each facility have comparable data sparsity (i.e., similar number of samples per square meter).

Statistical Comparison of Hazard Mapping with Static and Roving Monitors

In this study, the goal is to compare the difference between roving monitor estimates of the TWA noise intensity using short-duration measurements at each facility compared to the hazard map produced from static monitor TWAs. We

quantified differences between maps using two metrics. The first was the root mean squared error (RMSE), which was calculated from the difference in paired Leq estimates between separate hazard maps (roving and static (TWA) monitor data). The RMSE is an estimator of overall difference between maps to compare relative similarity. The second way differences were quantified was to determine the error rate, the fraction of interpolation locations (at 1 m^2 resolution) for which interpolated Leq values differed (from one map to the next) by more than 2 dBA or 5 dBA. These arbitrary threshold values were selected to give an indication of the proportion of the facility for which the roving monitor data provided a good estimate of the TWA.

For each facility and sampling day, the role of sampling resolution was assessed by randomly selecting N sampling locations from each full traverse, producing a hazard map and calculating the difference metrics. For the reduced resolutions, this process was repeated 1000 times and the mean and standard deviation of the map comparison metrics were calculated for each sampling resolution on each day for both facilities.

RESULTS

Noise Exposure

Static monitoring at the plastics facility resulted in mean Leq levels from 81–84 dBA across the three days of monitoring. Leq levels measured with the static monitors were approximately normally distributed over time as confirmed with a Shapiro-Wilks normality test. At the engine facility, the daily average Leq estimated from all static monitors and all times was approximately 81 dBA on both days. The Shapiro-Wilks tests indicated departure from normality even after log-transformation at this facility (all data were used without transformation). Although noise levels from a single source are expected to have normal (or log-normal) variation, the high variability in noise intensity levels observed over time may have resulted in sampling from multiple different normal distributions that did not cumulatively exhibit normality even after log-transformation.

Temporal and Spatial Variability from Static Monitors

The cumulative distribution functions (CDFs) of observed Leq values from static dosimeters were plotted to assess temporal and spatial variability of noise intensities at the plastics facility and engine facility in Figure 3 (Day 1 is shown for each facility; other days are similar). Each line represents the empirical CDF for one static dosimeter location. At the plastics facility, noise intensities varied strongly with location but not with time (steeply sloped curves). At the plastics facility the lines of the CDF were offset from one another, representing conserved spatial variability throughout the facility. Thus, short-duration noise intensity measures at the plastics facility should be representative of TWA exposures. At the engine facility, strong variability was observed both spatially and temporally (shallow slopes were observed in the CDFs). There was likely more than one distinct noise source because the CDF lines representing different sampling locations crossed one another. As such, at the engine facility, short-duration noise intensity measures may be less representative of TWA exposures.

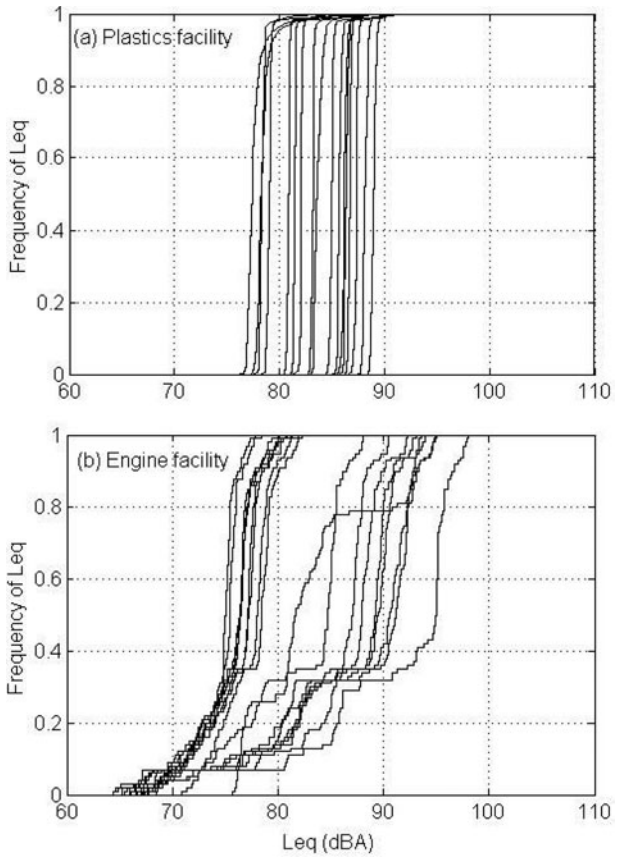

FIGURE 3. Empirical cumulative distribution function plots for noise intensity from static dosimeters are displayed for: (a) Day 1 at the plastics facility; (b) Day 1 at the engine facility.

Noise Hazard Mapping

The TWA hazard map from the noise intensity data collected with static monitors at the plastics facility (Day 1) is shown in Figure 4a. Because the noise source operates continuously at the plastics facility, the TWA hazard maps on Days 2 and 3 were very similar to Day 1 and are not shown here. The TWA hazard map identified two areas in the plastics facility with relatively higher sound pressure levels. We also plotted representative hazard maps from the roving monitors using all the data from one pass through the facility (Figure 4b) or a randomly selected subset of those data (Figure 4c–e). In each case, the roving data correctly identified the two regions of higher noise intensity. Peak intensities were often overestimated using the roving monitor data compared to the TWA and the extent of the high-intensity area varied depending on the density of the measurements (for hazard maps relying on a subset of sampling locations). The other traverse through

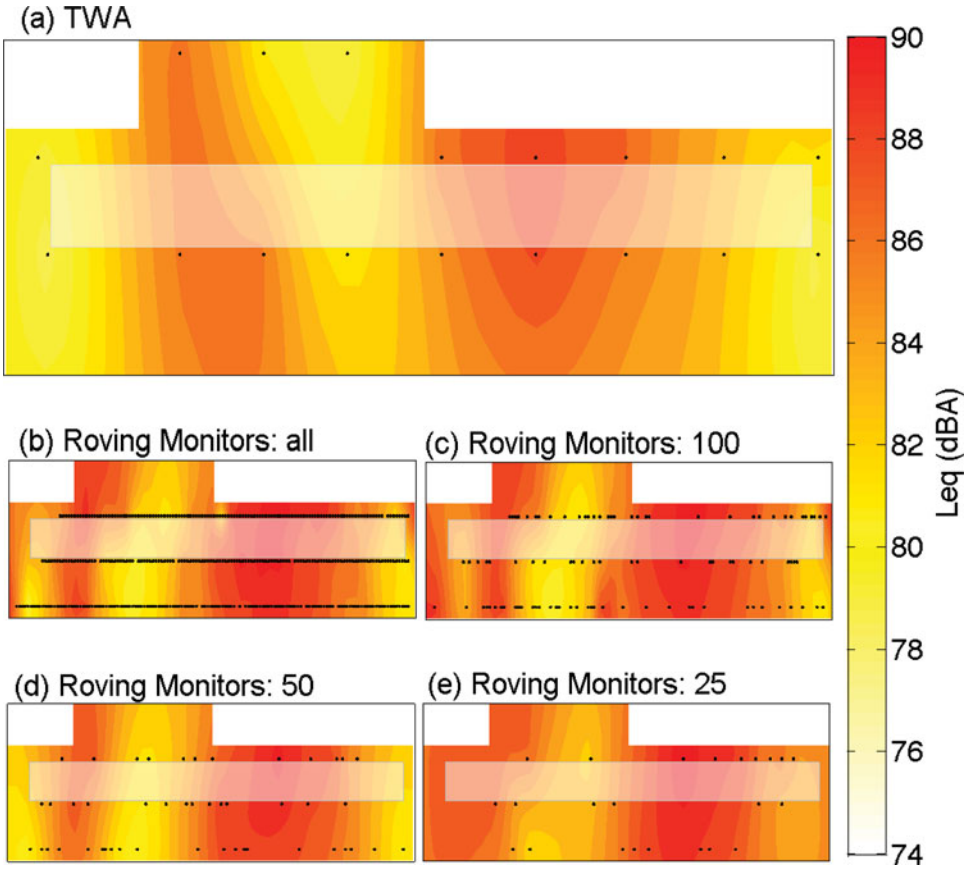

FIGURE 4. Hazard maps of noise intensity at the plastics facility on Day 1: (a) the TWA hazard map using data from the static monitors; (b) hazard map using all data from one traverse through the facility with the roving monitor; (c–e) a subset of 100, 50, or 25 randomly selected locations from the same traverse.

the facility (by the other researcher) resulted in similar hazard maps, as did the other two days of sampling.

On Day 1, two areas at the engine facility (the northwestern engine and southwestern corner) were identified with relatively higher TWA noise intensity levels, as seen in Figure 5a. The higher noise intensity in the southwestern corner was later identified as originating from nearby construction activities outside the building. Two researchers completed two traverses each through the facility (Figure 5b–c). Near the northwestern engine (an active noise source), the data from the roving monitors tended to overestimate the TWA noise intensity because measurements in this region happened to be completed during a high load portion of the engine testing. Additionally, because the outside noise source was intermittent and not anticipated, no roving measurements were completed in the southwest corner of the facility and the higher noise intensities in this region were missed by the roving sampling plan.

The TWA hazard map for Day 2 at the engine facility is shown in Figure 6a. The TWA map indicates that the region around the active engine in the engine facility had relatively higher noise intensity. Four replicate traverses (two each by two researchers) were made through the facility resulting in very different looking hazard maps (Figure 6b–e). The intensity near the active engine varied between different traverses and often overestimated the TWA intensity. Replicates 1 and 3 indicate low noise intensity at different regions of the facility likely resulting from temporal variability in the noise intensity that is portrayed as spatial variability by these maps.

We also produced videos of the hazard concentration as one-minute averages of the noise intensity measured by the static monitors at each facility on each day (see Online Supplemental Material). These videos again show the low temporal variability at the plastics facility (standard deviation of individual static monitors over time ranged from 0.2–1.5), increased temporal variability at the engine facility on Day 1 (standard deviation of individual static monitors over time ranged from 2.0–7.7), and even greater temporal variability at the engine facility on Day 2 (standard deviation of individual static monitors over time ranged from 7.2–10.8).

DISCUSSION

At the plastics facility, some differences were observed between the maps using the TWA and roving monitor

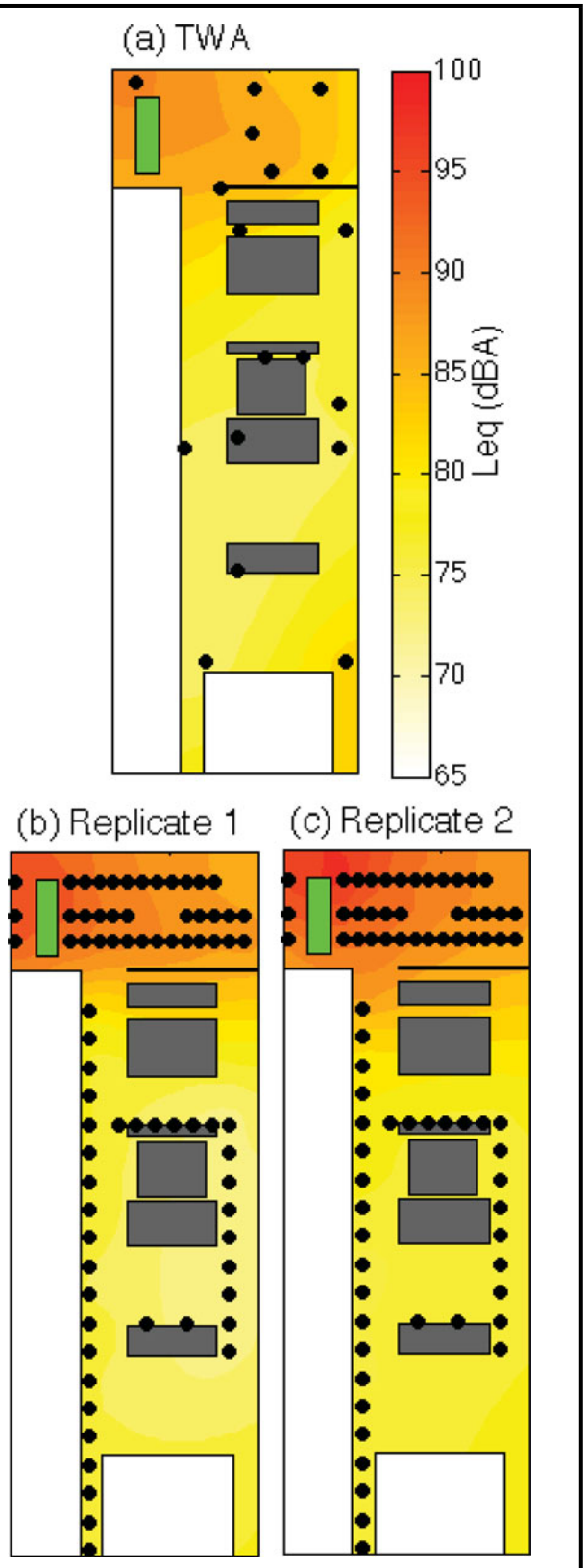

FIGURE 5. Hazard maps of noise intensity at the engine facility on Day 1: (a) the TWA hazard map using data from the static monitors; (b,c) hazard map using all data from two separate traverses through the facility with the roving monitor.

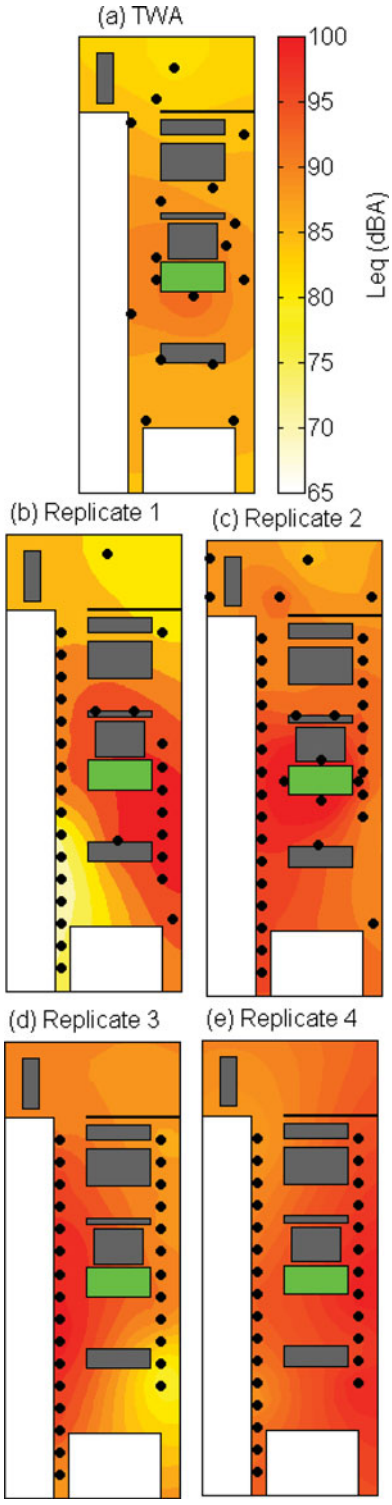

FIGURE 6. Hazard maps of noise intensity at the engine facility on Day 2: (a) the TWA hazard map using data from the static monitors; (b–e) hazard map using all data from four separate traverses through the facility with the roving monitor.

TABLE I. Accuracy of Hazard Maps Using the Roving Monitoring Data Compared to the Hazard Maps Using the TWA Data from Static Monitors at the Plastics Facility

Resolution	RMSE (×100)	Std (RMSE)	Error Rate > 2 dBA (%)	Error Rate >5 dBA (%)
			Day 1	
Full	3.03	0.47	52	5
100	2.83	0.27	49	2
50	2.81	0.33	48	2
25	2.85	0.45	46	5
Avg.	2.92	—	52	0
			Day 2	
Full	2.85	1.0	51	7
100	2.85	0.70	52	7
50	2.87	0.72	53	7
25	2.99	0.80	53	9
Avg.	2.69	—	51	6
			Day 3	
Full	3.29	0.75	54	11
100	3.22	0.50	54	10
50	3.13	0.56	52	10
25	3.09	0.63	50	10
Avg.	2.72	—	37	6

Notes: Root mean squared error (RMSE) and its standard deviation are shown in the first two columns. The second two columns are the error rate, the percentage of locations in the facility in which the value estimated using the roving monitoring data was at least 2 or 5 dBA different from the value estimated using the TWA data.

TABLE II. Accuracy of Hazard Maps Using the Roving Monitoring Data Compared to the Hazard Maps Using the TWA Data from Static Monitors at the Engine Facility

Resolution	RMSE (×100)	Std (RMSE)	Error Rate > 2 dBA (%)	Error Rate >5 dBA (%)
			Day 1	
Full	2.91	0.14	33	7
15	3.05	0.54	42	7
8	3.86	1.7	52	15
Avg.	2.91	—	5	0
			Day 2	
Full	7.0	0.45	81	54
15	7.2	0.97	83	58
8	7.4	1.57	84	61
Avg.	5.3	—	99	34

Notes: Root mean squared error (RMSE) and its standard deviation are shown in the first two columns. The second two columns are the error rate, the percentage of locations in the facility in which the value estimated using the roving monitoring data was at least 2 or 5 dBA different from the value estimated using the TWA data.

data particularly concerning the spatial extent of hazard concentrations, but the maps based on each data collection method (roving or static monitors) allowed successful identification of major sources of hazards and general areas of concern. At the plastics facility, noise intensities were homogeneous over time so sampling techniques with low temporal resolution were still representative of the TWA. To assess the extent of this difference, the RMSE between the TWA and the hazard maps produced from the roving monitor data was calculated as well as the error rate (at 1 m^{-2} resolution) with estimated noise intensities at least 2 dBA or 5 dBA different than the TWA for the plastics facility (Table I). The RMSE on each day was near 3% and the 2 dBA error rate covered approximately half of the locations. Far fewer locations were more than 5 dBA different (less than 11% of the facility).

The influence of sampling resolution did not have a clear trend. Thus, the relationship of noise intensity levels throughout the facility was likely well captured by the Kriging even when the spatial resolution of the measurements was quite low (25 locations in the facility equates to approximately 1 measurement every 78 m^2). The last row in Table I for each day uses noise intensity values that were averaged over replicate measures at each sampling location ("Avg." in Table I). In most cases only 2–3 replicates were taken per day at this facility, yet by averaging over even a small number of replicate samples, the comparability with the TWA hazard map was improved (i.e.,, generally reduced RMSE and error rate).

At the engine facility, noise intensity data collected from the roving monitors resulted in maps that diverged from the TWA map. To assess the extent of this difference at the engine facility (Table II), the RMSE between the TWA and the hazard maps produced from the roving monitor data was calculated as well as the error rate (at 1 m^{-2} resolution) with estimated noise intensities at least 2 dBA or 5 dBA different than the TWA. On Day 2, the temporal variability in noise intensity resulted in less precise estimates of the TWA when using the roving monitoring sampling plans. On that day, the error rate exceeded 5 dBA for over half of the facility. On both days at the engine facility, reducing the sampling resolution of the roving monitoring strategy, reduced the accuracy (larger and more variable RMSE) of the noise hazard maps. The reduced accuracy of the hazard maps generated with data from the roving sampling plan was likely caused by high temporal variability in noise intensities over time at the engine facility and random chance concerning when the sampling was conducted (compare maps 6b and 6d). More complete hazard maps at facilities with high variability noise sources likely requires sampling techniques with higher temporal resolution and with higher spatial resolution, to a lesser effect. However, averaging over replicate measures at a location again improved

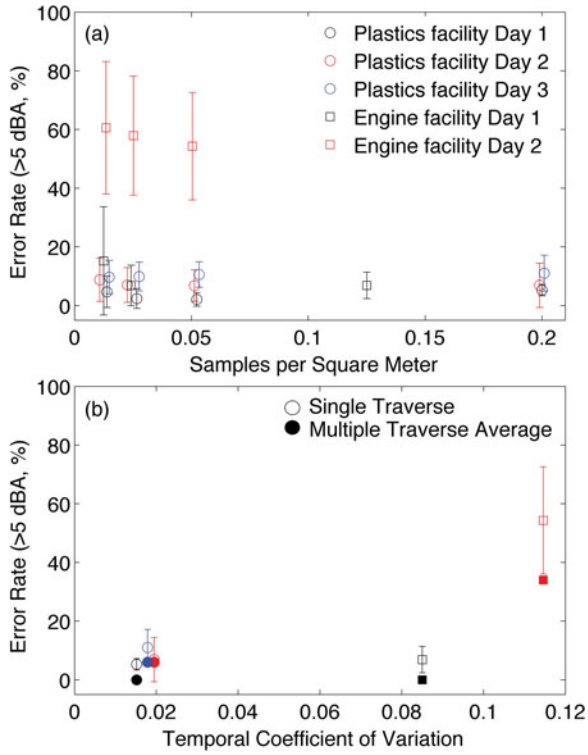

FIGURE 7. Error rate (the fraction of interpolation locations for which interpolated Leq values differed from the roving monitoring data map to the TWA map by more than 5 dBA) as a function of: (a) the number of samples per square meter (values jittered slightly for clarity); (b) the coefficient of variation of the most variable static monitor (colors and symbols as in part (a); open symbols represent a single traverse through the facility; filled symbols represent the average of all traverses through the facility). Error bars represent one standard deviation of the error rate from 1000 replicates of random subset sampling for the reduced spatial resolutions or one standard deviation of the replicate traverses through the facility at full spatial resolution.

the performance of the hazard maps generated with roving monitoring data compared to the TWA.

The importance of spatial resolution and temporal variability on the ability of the roving monitors to estimate the TWA map is displayed in Figure 7. The 5 dBA error rate was plotted as a function of spatial resolution (sampling points per square meter, Figure 7a) and temporal coefficient of variation (standard deviation over time for the most variable static monitor divided by its temporal mean intensity, Figure 7b). The error bars in Figure 7 represent one standard deviation of the error rate from 1000 randomly selected data subsets or one standard deviation of the replicate traverses through the facility at full spatial resolution (right-most point for each facility and sampling day in Figure 7a). The influence of spatial resolution was small at the plastics facility; the error rate was nearly constant with increasing spatial resolution. However, the error rate decreases with increasing spatial resolution at the engine facility (Figure 7a).

At both the plastics facility and the engine facility, the standard deviation about the error rate decreased as the spatial resolution increased, suggesting that increasing the spatial resolution of the measurements improves the reliability of the hazard map interpolation. The influence of temporal variation on map comparability was much stronger than the spatial resolution when the data from both facilities were compiled (Figure 7b, full spatial resolution shown). At the plastics facility, the temporal variability was low and the error rate was correspondingly low. The error rate increased with increased temporal variability at the engine facility. The increasing error rate likely reflects that temporal variability can be misrepresented as spatial variability when a single traverse through the facility is completed. When the temporal coefficient of variation is less than ~0.1, few measurements (in both time and space) are likely sufficient to adequately capture the TWA hazard map. At higher levels of temporal variability it can be beneficial to complete replicate measurements at the sampling locations. The error rate when all replicate traverses through the facility were averaged is plotted as filled symbols in Figure 7b. In all cases the error rate decreased when replicate measurements were averaged; this sampling strategy may prove more beneficial than increasing the spatial resolution of the measurements.

Our results suggest that as temporal variability increases, roving monitoring data are less capable of accurately estimating the spatial variability of the TWA exposures; however, based on data from two facilities the functional relationship between temporal variability and map accuracy is unclear. Future work should examine the relationship between temporal variability of hazards and the accuracy of roving monitors used to estimate mapped TWA exposures. For future hazard mapping analyses, we recommend that preliminary data on the temporal variability of hazard intensity at a facility (measured near a source expected to have the highest temporal variability) be collected. The temporal coefficient of variation among the preliminary data can suggest whether bias is anticipated and whether certain sampling strategies can be employed (such as including replicate measurements) to improve the estimation of the TWA hazard map.

Few studies have deployed static monitors with enough spatial resolution to capture the spatial variability in TWA concentrations in an occupational facility. Several studies have deployed direct-reading units to capture temporal variability at one or two locations (for example, references [8,14]; however, those measurements were not used to inform the mapping analyses. Liu and Hammond [15] assessed temporal variability during 10-minute intervals at seven locations to inform their roving sampling strategy and concluded that high temporal variability, even during relatively steady-state operations, likely limited the ability to represent TWA concentrations by short-duration measurements during mapping. Peters et al. [6] monitored particulate mass concentrations at a five locations in a swine gestation facility. The geometric mean and 84th percentile mass concentrations in the

facility were estimated from both mapped concentrations using short-duration measurements and from the five static monitors. Differences between these two estimates ranged from 7% to 46%. These authors did not produce hazard maps from the static monitors, thus it is unclear if there were differences in the spatial patterns of exposure from the two data collection methods.

CONCLUSION

Hazard mapping was conducted at a plastic manufacturing facility and an engine testing facility. Analysis of static noise dosimeters at the plastics facility revealed homogeneous noise intensity levels over time. Our results suggest that at facilities with homogeneous noise intensities over time, the similarity between hazard maps produced from static and roving monitoring methods will be high. At the engine facility, analysis of static noise dosimeters revealed highly variable noise intensity levels over time and space. With higher levels of spatial and temporal variability, hazard maps produced with data from static and roving monitoring methods were substantially different.

Future studies using roving monitoring to assess the spatial extent of hazards in workplaces should consider the temporal variability of the hazard. At facilities with higher temporal variability, hazard maps will be useful to capture transient, high-level exposures that are missed by standard TWA methods. However it is important to remember that these maps may be biased compared to the TWA value and replicate measures should be taken to improve map accuracy. Further, computer simulation studies should be conducted to more rigorously evaluate various sampling strategies and spatial/temporal variability, which we leave for future investigation.

FUNDING

This work was funded in part by grant #5K01OH009886 from the National Institute for Occupational Safety and Health (NIOSH).

SUPPLEMENTAL MATERIAL

Supplemental data for this article can be accessed at tandfonline.com/uoeh. AIHA and ACGIH members may also access supplementary material at http://oeh.tandfonline.com/.

REFERENCES

1. **National Institute of Occupational Safety and Health (NIOSH)**: *Work Related Hearing Loss*. Atlanta: NIOSH, 2001.
2. **Hong, O.S.**, **M.J. Kerr**, **G.L. Poling**, **et al.**: Understanding and preventing noise-induced hearing loss. *Dis. Mon. 59*(*4*):110–118 (2013).
3. **Metwally, F.M.**, **H.M. Aziz**, **H. Mahdy-Abdallah**, **et al.**: Effect of combined occupational exposure to noise and organic solvents on hearing. *Toxicol. Ind. Health 28*(*10*):901–907 (2012).
4. **Campo, P.**, **T.C. Morata**, and **O.S. Hong**: Chemical exposure and hearing loss. *Dis. Mon. 59*(*4*):119–138 (2013).
5. **Koehler, K.A.**, and **T.M. Peters**: Influence of analysis methods on interpretation of hazard maps. *Ann. Occup. Hyg. 57*(*5*):558–570 (2013).
6. **Peters, T.M.**, **T.R. Anthony**, **C. Taylor**, **et al.**: Distribution of particle and gas concentrations in swine gestation: Confined animal feeding operations. *Ann. Occup. Hyg. 56*(*9*):1080–1090 (2012).
7. **Evans, D.**, **W. Heitbrink**, **T. Slavin**, and **T. Peters**: Ultrafine and respirable particles in an automotive grey iron foundry. *Ann. Occup. Hyg. 52*(*1*):9 (2008).
8. **Peters, T.M.**, **W.A. Heitbrink**, **D.E. Evans**, **et al.**: The mapping of fine and ultrafine particle concentrations in an engine machining and assembly facility. *Ann. Occup. Hyg. 50*(*3*):249–257 (2006).
9. **Ologe, F.E.**, **T.M. Akande**, and **T.G. Olajide**: Occupational noise exposure and sensorineural hearing loss among workers of a steel rolling mill. *Eur. Arch. Oto-Rhino-Laryngol. 263*(*7*):618–621 (2006).
10. **O'Brien, D.M.**: Aerosol mapping of a facility with multiple cases of hypersensitivity pneumonitis: Demonstration of mist reduction and a possible dose/response relationship. *Appl. Occup. Env. Hyg. 18*:947–952 (2003).
11. **Koehler, K.A.**, and **J. Volckens**: Prospects and pitfalls of occupational hazard mapping: 'Between these lines there be dragons'. *Ann. Occup. Hyg. 55*(*8*):829–840 (2011).
12. **Royster, L.**, **E. Berger**, and **J. Royster**: Noise Surveys and Data Analysis. In *The Noise Manual*, E. Berger, L. Royster, J. Royster, et al. (eds.). Fairfax, VA: American Industrial Hygiene Association, 2003. pp. 165–244.
13. **Cressie, N.A.C.**: *Statistics for Spatial Data*. New York: J. Wiley, 1993.
14. **Dasch, J.**, **J. D'Arcy**, **A. Gundrum**, **et al.**: Characterization of fine particles from machining in automotive plants. *J. Occup. Env. Hyg. 2*(*12*):609–625 (2005).
15. **Liu, S.**, and **S.K. Hammond**: Mapping particulate matter at the body weld department in an automobile assembly plant. *J. Occup. Env. Hyg. 7*(*10*):593–604 (2010).